

# Worldline deconfinement and emergent long-range interaction in entanglement Hamiltonian and entanglement spectrum

Zenan Liu,<sup>1,2</sup> Zhe Wang,<sup>1,2</sup> Dao-Xin Yao,<sup>3,\*</sup> and Zheng Yan<sup>1,2,†</sup>

<sup>1</sup>*Department of Physics, School of Science and Research Center for Industries of the Future, Westlake University, Hangzhou 310030, China*

<sup>2</sup>*Institute of Natural Sciences, Westlake Institute for Advanced Study, Hangzhou 310024, China*

<sup>3</sup>*State Key Laboratory of Optoelectronic Materials and Technologies, Guangdong Provincial Key Laboratory of Magnetoelectric Physics and Devices, Center for Neutron Science and Technology, School of Physics, Sun Yat-Sen University, Guangzhou 510275, China*

(Dated: June 16, 2025)

When a system exhibits a bulk gap but gapless edge states (e.g., a symmetry-protected topological phase), the entanglement spectrum (ES) resembles the energy spectrum on virtual edge, that is the Li-Haldane conjecture. In this way, the ES plays an important probe to detect the topological phases according to this bulk-edge correspondence. When a system is fully gapped, both in bulk and edge, the ES still remains similar to the virtual edge spectrum which can be explained by the recently proposed wormhole effect in the path integral of reduced density matrix. However, what will happen in the ES when the system is fully gapless? We find that though the ES roughly seems like an edge energy spectrum, and it actually contains relevant long-range interaction which modifies the intrinsic physics of entanglement Hamiltonian (EH). Moreover, the mechanism of short-/long-range interaction in EH can be understood as the confinement/deconfinement of worldlines in a path integral of reduced density matrix. Our work demonstrates that the gapless mode can induce a long-range interaction in EH.

## I. INTRODUCTION

Entanglement is a unique and important concept in many-body physics, which has become a powerful tool to understand the topology and categorical symmetries of condensed matters [1–13]. Its application also extend to the conformal field theory (CFT) [14, 15], quantum field theory, and quantum information [16–19]. Commonly, the entanglement entropy (EE) is widely used to probe various phases and phase transitions, which can also capture the universal properties and anomaly of systems, such as continuous symmetry breaking, ground state degeneracy and critical behaviors [11, 12, 20, 21]. In the topological phases, EE can reveal the topological features and quantum dimension of topological excitation via scaling behaviors [11, 18, 22, 23].

In addition, entanglement spectrum (ES) was proposed to extract the universal feature and CFT information of topological ordered phase, capturing more information than EE [24–41]. Hui Li and Haldane firstly proposed that the low-lying entanglement spectrum will be similar to the edge energy spectrum on the physical boundary in the topological phase, dubbed as Li-Haldane conjecture [42]. Their work demonstrated that the general  $\nu = 5/2$  quantum fractional Hall states have the same low-lying ES with topological structure. Then, it was theoretically proved that there is a general correspondence between the entanglement spectrum of  $(2+1)d$  chiral gapped topological states and energy spectrum on

$(1+1)d$  edges [27]. Following numerical results also show that this conjecture still holds in many magnetic systems including topological state [34, 43–48].

For a system with gapped bulk and gapless edge, such as the symmetry-protected topological (SPT) phase, the EH is generally believed to be short-range corresponding to the virtual edge Hamiltonian, known as the famous Li-Haldane conjecture [42, 49]. Sometimes, although the EH contains the long-range interaction, these exponentially decaying long-range terms are irrelevant. In such case, the ES still resembles the edge spectrum [50–55]. Because the long-range interaction can be ignored, the EH retains physical properties similar to virtual edge Hamiltonian. The conclusion also holds when both bulk and edge are gapped, supported by the numerical evidence and wormhole effect in the path integral of reduced density matrix [47]. All the above conclusions are based on a bipartite entangled-cut, in which the reduced system has both bulk and edge. When we split a ladder/bilayer system into two chains/layers by entangled-cut, gapped system can even emerge a long-range interacting EH [56–58]. Thus we restrict the discussion of this work in the first condition, that is, a bipartite entangled-cut with both bulk and edge.

A natural question is what will happen to the EH when the system is fully gapless. Field theory analysis suggests that the EH in binary Bose-Einstein condensates may exhibit relevant long-range interactions [50]. In physical systems described by original Hamiltonians, extensive studies have shown that strong long-range interactions can fundamentally alter intrinsic physics, even violating the Mermin-Wagner theorem [59, 60]. For instance, they may change the dispersion power in continuous symmetry

\* yaodaox@mail.sysu.edu.cn

† zhengyan@westlake.edu.cn

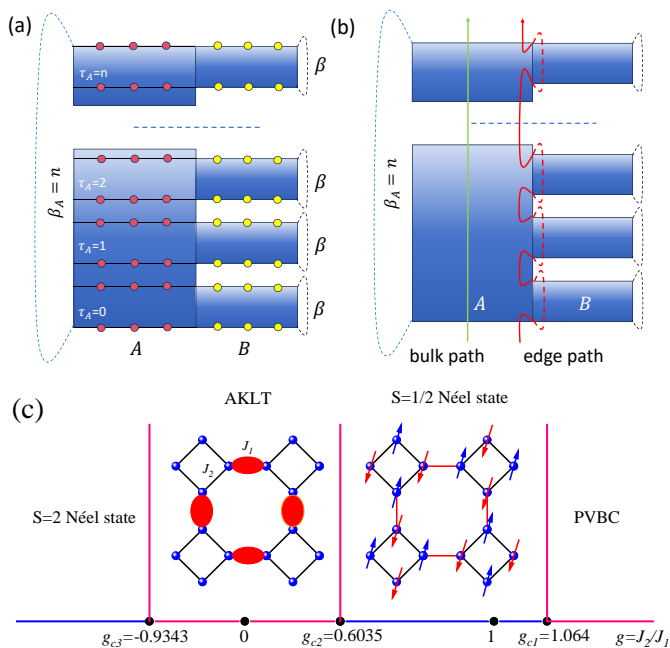


FIG. 1. (a) The replica manifold in the QMC simulation. (b) The diagram for wormhole mechanism. (c) The phase diagram for spin-1/2 Heisenberg model on the square-octagon lattice. We mainly focus on the AKLT phase and Néel phase.

systems [61–63] or open a gap of an original Goldstone mode [61, 64, 65]. Therefore, the feature of spectrum can serve as an indicator of whether long-range interactions are relevant. But it is still a challenging task for numerical methods to extract the large scale spectrum of EH in (2+1)d system.

Here, we utilize a newly developed quantum Monte Carlo (QMC) method simulating the path integral of reduced density matrix [44, 47] to reveal the importance of long-range interaction in the ES by taking a two-dimensional Affleck-Kennedy-Lieb-Tasaki (AKLT) model as an example. When the bulk is at the quantum critical point and in the Néel phase, we observe the ES exhibits a M-shape magnon with sublinear dispersion rather than linear dispersion. This change of ES is similar to the excitation spectrum in the one-dimensional  $S = 1/2$  Heisenberg chain with long-range interaction, which can be confirmed in our QMC simulation. The long-range interaction leads to the sublinear dispersion with power  $s \sim 0.2$  in the Néel state, which is not consistent with the linear dispersion of energy spectrum. Further, we demonstrates that the mechanism can be understood by the deconfined worldlines created along the gapless mode.

## II. MODEL AND METHOD

*Model.*- We investigate the  $S = 1/2$  Heisenberg model on the square-octagon lattice via quantum Monte Carlo,

dubbed as two-dimensional AKLT model [66, 67].

$$H = J_1 \sum_{\langle ij \rangle} \mathbf{S}_i \cdot \mathbf{S}_j + J_2 \sum_{\langle ij \rangle'} \mathbf{S}_i \cdot \mathbf{S}_j \quad (1)$$

where  $J_1$  is the inter-unit cell interaction and  $J_2$  is the intra-unit cell interaction. We define  $g = J_2/J_1$  with  $J_1 = 1$ . The model can host a rich phase diagram including  $S = 2$  Néel phase, AKLT phase,  $S = 1/2$  Néel phase and plaquette valence bond crystal (PVBC). The detailed phases and phase diagram can be found in Ref. [67]. These phases are separated by three quantum critical points which all belong to (2+1)d  $O(3)$  universality class, as shown in Fig.1(c). In the AKLT phase, the boundary can be described by an effective  $S = 1/2$  Heisenberg chain which hosts gapless two-spinon continuum excitation [68]. At bulk quantum critical point, the boundary can induce exotic surface critical behaviors due to the coupling between edge mode and bulk critical mode [69].

*Method.*- We use a newly proposed QMC method to extract the large-scale ES of two-dimensional AKLT model. As we know, the reduced density matrix (RDM)  $\rho_A = \text{Tr}_{\bar{A}}(|\psi\rangle\langle\psi|) = e^{-\mathcal{H}_A}$  can not be directly calculated via QMC simulation, though it is easy for ED and DMRG to implement. Here, the  $A$  is the subsystem and  $\bar{A}$  is the environment,  $\mathcal{H}_A$  is the corresponding entanglement Hamiltonian for subsystem. Via the replica method [44], we introduce an effective imaginary-time  $n$  for entanglement Hamiltonian and get the effective partition function of EH  $\mathcal{H}_A$  as follows,

$$\mathcal{Z}_A^{(n)} \propto \text{Tr}[\rho_A^n] = \text{Tr}[e^{-n\mathcal{H}_A}] \quad (2)$$

where the replica number  $n$  can be treated as the effective imaginary-time length  $\tau_A$  for EH (distinguished from normal  $\tau$ , this  $\tau_A$  is for EH only), as shown in Fig.1 (a). The imaginary-time correlation of  $\mathcal{H}_A$  can be obtained by measuring the  $G(\tau_A, \mathbf{q}) = \langle O_{-\mathbf{q}}^\dagger(\tau_A) O_{\mathbf{q}}(0) \rangle$ , where  $\tau_A$  is the imaginary time for EH (the number of replica) and  $\mathbf{q}$  is the momentum. Then, we can extract the operator  $O$  of spectral function  $G(\omega, \mathbf{q})$  for the EH via stochastic analytic continuation (SAC) for the corresponding imaginary-time correlation [70–73]. Due to the translation symmetry and spin rotation symmetry, we focus on the boundary imaginary-time correlation function for the  $s^z$  operator,  $G(\tau_A, q) = \frac{1}{L} \sum_{i,j} e^{-iq \cdot (x_i - x_j)} \langle s_i^z(\tau) s_j^z(0) \rangle$ , where  $s_{i(j)}^z$  denotes spins on the entanglement boundary.

*Wormhole picture.*- The new QMC method also gives a new insight to understand the relationship between energy spectrum and entanglement spectrum. In the replica manifold as shown in Fig.1 (a) and (b), the trace of environment actually connects the upper and lower edge of replica as a periodic boundary condition (PBC) in imaginary-time direction. Thus it can provide a convenient way for worldlines near entangled edge to get to the upper edge from the lower edge very fast, dubbed as wormhole picture. It make worldlines near entangled edge avoid crossing the bulk of replica with huge cost as worldlines in the depth of bulk.

In the frame of path integral, the cost is roughly proportional to the product of time-length and Hamiltonian gap on this path  $\bar{\mathcal{L}} \times \Delta(\bar{\mathcal{L}})$ , where  $\bar{\mathcal{L}}$  is the average path length of imaginary time and  $\Delta(\bar{\mathcal{L}})$  is the average gap for this path. The smaller cost will lead the larger path weight which can give greater contribution to the low-lying ES. Because the time-length in one replica is equal to  $\beta$  and the time-length around entangled edge can be treated as a constant 1 due to the wormhole effect, the ratio between the bulk path and edge path is roughly  $\beta : 1$ .

When considering the path length and gap synthetically, the ratio of cost between bulk path and edge path can be estimated roughly as  $\beta\Delta_b : \Delta_e$ , where  $\Delta_b$  is the bulk gap and  $\Delta_e$  is the edge gap.  $\beta$  should go to  $\infty$  in the ground state which renders  $\beta\Delta_b \gg \Delta_e$ . Then the cost of edge path is much lower than the bulk path. The edge mode will have a larger weight and contribute more information to the low-lying ES. Therefore, the entangled edge mode in EH is gapless as a virtual edge mode in the original Hamiltonian with open boundary condition, the Li-Haldane conjecture can be well explained via wormhole picture [44].

However, when the system is gapless, both  $\Delta_b$  and  $\Delta_e$  are 0, the wormhole picture loses the effectiveness where the length of imaginary time path is irrelevant. We need to carefully calculate whether the worldlines are deconfined or confined in the path integral to detect the real costs of different paths.

### III. ENTANGLEMENT SPECTRUM

We investigate the evolution of entanglement spectrum when the system is from AKLT phase to  $S = 1/2$  Néel phase. The system size  $L$  is 32 with  $\beta_A = 64$  and  $\beta = 50$ . When  $g = 0.4 < 0.6035$ , the system is in the deep AKLT phase. The ES is a gapless two-spinon continuum excitation, which is similar to the edge energy spectrum, as shown in Fig.2(a). In this phase, the boundary can be considered as an effective Luttinger Liquid. When the  $g$  becomes larger but still in the AKLT phase, such as  $g = 0.5, 0.55$ , the spinon continuum seems weaker but it is hard to judge whether it is disappeared. As  $g$  goes to the critical point  $g_c = 0.6035$ , the spectrum resembles a sharp dispersion with possible gap in the rough precision. There may be questionable long-range interactions in EH here, but it is difficult to make a definite conclusion from a spectroscopic perspective.

When  $g$  further increases, we observe that the two-spinon continuum obviously disappears. The ES becomes sharp magnon, which reflects that the bulk undergoes the quantum phase transition between AKLT phase and Néel phase. However, the dispersion near the  $q = \pi$  becomes not linear as shown in Fig.2(d)-(f), which is not like the edge excitation in the Néel state with open boundary. In the previous work [68], the real edge excitation is a gapless linear dispersion. Moreover, the gap near  $q = \pi$

looks larger and larger as  $g$  increases, which indicates that the ES may become discontinuous and opens a gap at  $q = \pi - \frac{2\pi}{L}$  (Fig.2(d)-(f)). As the bulk undergoes the phase transition, the length of the entanglement will increase. The short-range nature of entanglement Hamiltonian will gradually change as bulk approaches the criticality. Therefore, the effective model for the subsystem should be no longer a short-ranged Hamiltonian, and the long-range interaction will be induced and become important.

When  $g > g_c$ , the ES seemingly opens a gap at  $q = \pi - \frac{2\pi}{L}$ , which is mainly caused by the relevant long-range interaction. This similar phenomenon can be also found in the two-dimensional Heisenberg model with long-range interaction on the square lattice [61, 63]. These studies suggest that the entanglement Hamiltonian in the Néel phase can be effectively modeled as a Heisenberg chain with long-range interactions along the entanglement boundary. To further investigate the impact of long-range interaction on the spectrum, we consider an one-dimensional  $S = 1/2$  antiferromagnetic Heisenberg chain with power-law long-range interaction. This model allows us to systematically explore how long-range interactions influence the entanglement properties and spectral behaviors. This Hamiltonian is written as

$$H = \sum_i \sum_{r \geq 1} J_r \mathbf{S}_i \cdot \mathbf{S}_{i+r} \quad (3)$$

where  $J_r = (-1)^{r-1}/r^\alpha$  without sign problem for QMC simulation. When  $\alpha \rightarrow \infty$ , this Hamiltonian becomes short-ranged Heisenberg chain whose ground state is Luttinger liquid. When  $\alpha < 3$ , the linear dispersion will break down due to the long-range interaction. As  $\alpha$  gradually decreases, the long-range interaction will induce a long-range order. At  $\alpha \approx 2.23$ , the system will undergoes a quantum phase transition between the Néel phase and Luttinger liquid phase [74, 75]. When  $\alpha < 2.23$ , the long-range interaction becomes relevant and drives the system into the long-range Néel order [76, 77]. If  $\alpha < 1$ , the spin excitation spectrum will become discontinuous and open a gap near  $q = \pi$ , which enters the super long-range phase and falls in the fully connected Lieb-Mattis case [75, 78].

We extract the spin excitation spectrum of this model via QMC and SAC. When  $\alpha$  is large, the system is a Luttinger Liquid phase which hosts gapless two spinon continuum excitation. As  $\alpha$  decreases, the long-range interaction will suppress the two-spinon continuum and make it confined. As the system enters the Néel phase, magnon excitation becomes dominant [79]. In order to benchmark the numerical results, we use the linear spin wave theory to obtain the low energy dispersion of long-range Heisenberg chain. Assuming the ground state is ordered, we utilize the Holstein-Primakoff (HP) transformation to transform the spin operators at the linear-wave level. The transformation can be expressed in terms of the boson creation and annihilation operators,  $S_i^z = S - a_i^+ a_i$ ,  $S_i^+ \approx \sqrt{2S} a_i$ ,  $S_i^- \approx \sqrt{2S} a_i^+$ , and

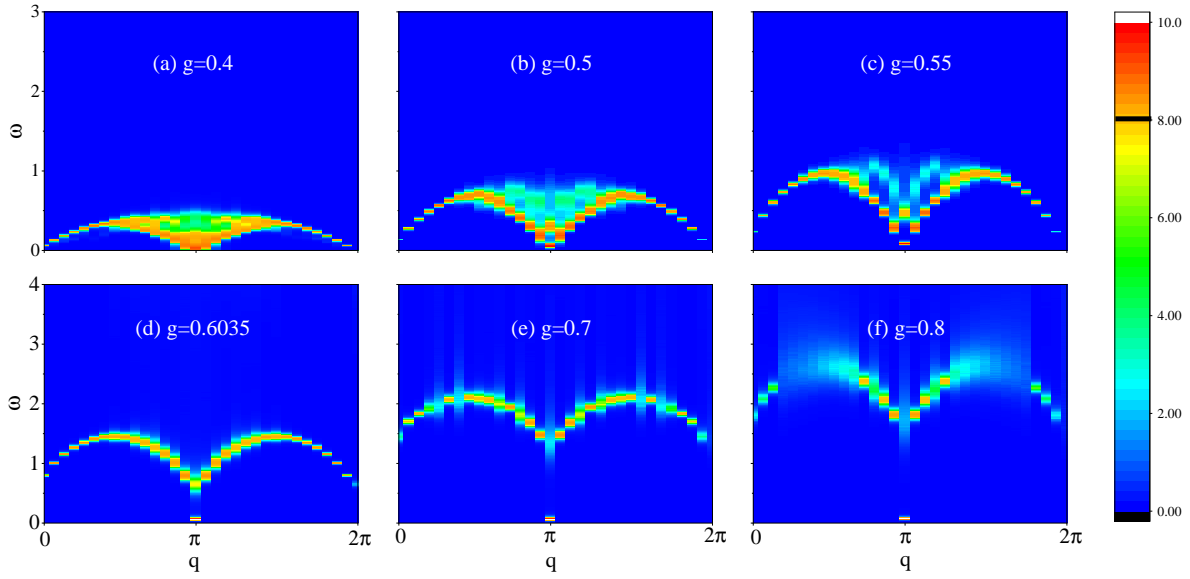


FIG. 2. Entanglement spectrum for AKLT state and Néel state.  $g$  is 0.4(a), 0.5(b), 0.55(c), 0.6035(d), 0.7(e), 0.8(f).

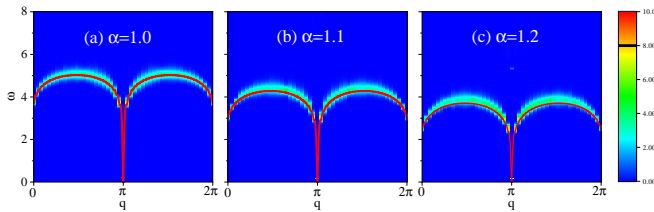


FIG. 3. Spin excitation spectra for one-dimension Heisenberg chain with long-range interaction for  $L = 48$  and  $\beta = 96$ . The power law of long-range interaction  $\alpha = 1.0$ (a), 1.1(b) and 1.2(c)

$S_j^z = b_j^+ b_j - S$ ,  $S_j^+ \approx \sqrt{2S} b_j^+$ ,  $S_j^- \approx \sqrt{2S} b_j$ , where  $a_i^+$  and  $a_i$  are for up spins and  $b_j^+$  and  $b_j$  are for down spins. Then, we obtained the spin wave Hamiltonian  $H_{sw}$  via HP transformation. By the Fourier transformation and numerical diagonalization for  $H_{sw}$ , we can extract the spin wave dispersion of the system. As Fig.3 shows, the spin wave theory is well consistent with the QMC+SAC results in the Néel state of the long-range interacting chain ( $\alpha < 2.23$ ), while it can not capture the low-energy dispersion in the Luttinger liquid phase ( $\alpha > 2.23$ ).

However, the dispersion is not always linear and gapless near  $q = \pi$ . In the Néel phase, the dispersion also becomes nearly discontinuous, which is similar to the ES of 2D AKLT model as shown in Fig.2 and Fig.3. According to the spin wave theory, the dispersion relation near  $q = \pi$  takes the sublinear form as,

$$\omega(q) \propto |q - \pi|^{\frac{(\alpha-1)}{2}} (\alpha < 3) \quad (4)$$

where power  $s = (\alpha - 1)/2$  according to the spin-wave theory [74]. Also, the dispersion relation takes the similar form as  $\omega(q) \propto |q|^{\frac{(\alpha-1)}{2}}$  near  $q = 0$ . It may take the

similar sublinear form in the ES of Néel phase. When  $\alpha = 1$ , the dispersion power  $s = (\alpha - 1)/2$  is equal to zero, which indicates the spectrum open a gap near  $q = \pi$  in Fig.3(a). These results demonstrate that the effective model for the subsystem near the entanglement boundary can be described by one-dimensional Heisenberg chain with relevant long-range interaction ( $\alpha$  is small).

From the Fig.2, it is unclear whether the gap at  $q = \pi - 2\pi/L$  is open in the thermodynamic limit. In order to solve this confusion, we extract the dispersion power  $s = (\alpha - 1)/2$  and the ES gap near  $q = \pi$  with different system size  $L$ . We define  $\Delta q = q - \pi$  and fit the dispersion power  $s$  via the formula  $\omega \propto |\Delta q|^s$ . As Fig.4(a)-(c) illustrates, we observe the dispersion near  $q = \pi$  satisfies the Eq.(4) with power  $s < 1$  in the Néel phase. At  $g=0.7$  and  $0.8$ , the dispersion power  $s \sim 0.2$ , which indicates that the long range interaction strongly modifies the dispersion. We also extract the dispersion power  $s$  of different system size  $L$  and perform the finite size scaling of  $s$  at Fig.4(d). Actually, the dispersion  $s$  converge to a constant as  $s(L) = s(\infty) + bL^{-1} + O(L^{-2})$ , where  $s(\infty)$  is the dispersion power in the thermodynamic limit and  $b$  is the fitting parameter. By fitting the data, we obtain the extrapolation of dispersion  $s(\infty) = 0.3915(2)$  for  $g = 0.6035$ ,  $0.2016(7)$  for  $g = 0.7$  and  $0.211(2)$  for  $g = 0.8$ . According to the dispersion relation for 1D Heisenberg chain with long-range interaction, we can roughly estimate that  $\alpha$  for EH should be smaller than 2.23, which demonstrates that long-ranged term is relevant.

In order to confirm whether the ES open a gap near  $q = \pi$  in the thermodynamic limit, we further explore the finite size scaling of ES gap at  $q = \pi - 2\pi/L$ . In Fig.4, it seems that the the ES gap is large with strong finite size effect. If we use the polynomial function (with 2, 3

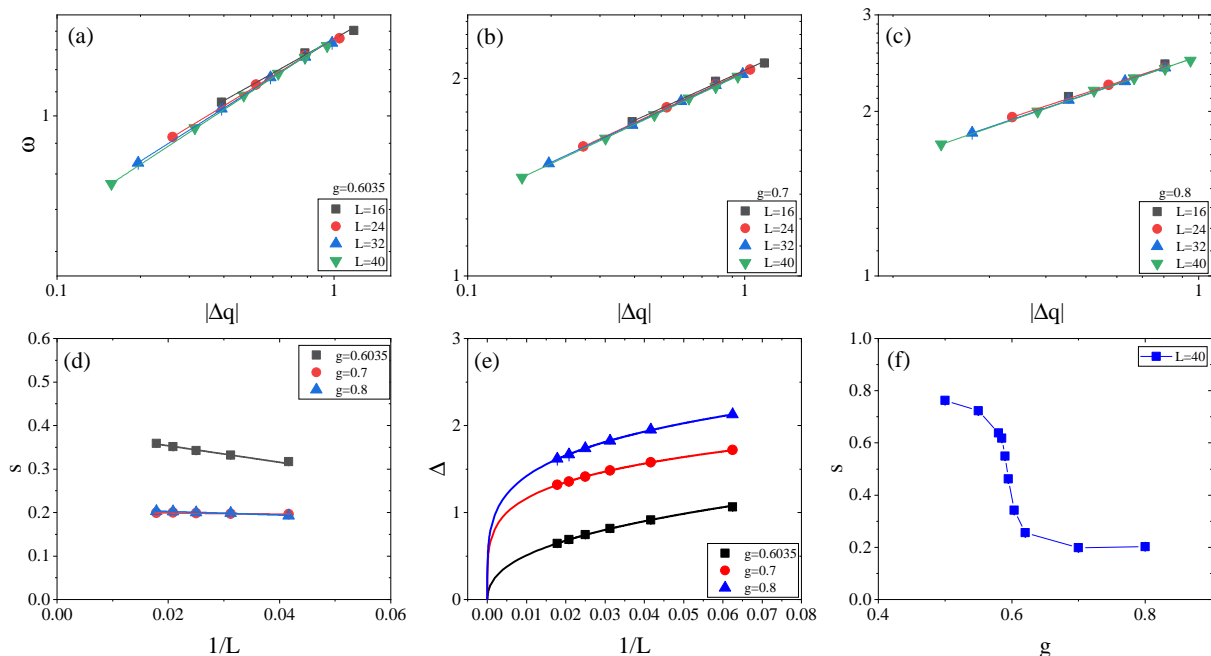


FIG. 4. Extracting the dispersion power  $s$  from the dispersion curve with different  $g$ . (a)-(c): The dispersion curve obtained from QMC simulation with different  $g$ . (d) Finite size scaling of the dispersion power  $s$  fitting from (a)-(c), we fit the power  $s$  by  $\omega = a|\Delta q|^s$ . (e) Finite size scaling of the entanglement gap  $\Delta(q = \pi - 2\pi/L)$  at  $q = \pi - 2\pi/L$ . We use the function  $\Delta = aL^s + \Delta(\infty)$  to fit the data with  $s = 0.3915$  ( $g = 0.6035$ ),  $0.2016$  ( $g = 0.7$ ) and  $0.211$  ( $g = 0.8$ ). (f) Finite size scaling of the dispersion power  $s$  for different  $g$  with system sizes  $L = 40$ .

and 4 order) to fit the finite size of ES gap, it converges to a positive constant as  $L \rightarrow \infty$ , which indicates the ES open a gap at  $q = \pi - 2\pi/L$ . But the scaling should satisfy the power-law  $\Delta(L) = aL^s + \Delta(\infty)$ , where  $\Delta(\infty)$  is the gap and  $s$  is the dispersion power in the thermodynamic limit. Because the dispersion is much smaller than 1, the scaling should not hold the polynomial form. When we use the power law form with  $s = 0.3915$  to fit the data of  $g = 0.6035$ ,  $\Delta(\infty) = -0.036(11)$  close to zero, as Fig.4(e) depicts. For  $g=0.7$  and  $0.8$ , we obtain  $\Delta(\infty) = -0.077(15)$  and  $-0.081(22)$  smaller than 0 (suppose  $s = 0.216$  ( $g = 0.7$ ) and  $0.211$  ( $g = 0.8$ )), which demonstrates that it will converge to zero at slow speed and keep gapless in the thermodynamic limit (Fig.4(e)). Besides, if we suppose the  $\Delta(\infty) = 0$  and use the form  $\Delta = aL^s$  to fit the data, we can also extract the dispersion  $s = 0.4086(1)$  ( $g = 0.6035$ ),  $0.2124(6)$  ( $g = 0.7$ ) and  $0.221(1)$  ( $g = 0.8$ ), which is close to the extrapolation value in Fig.4 (d). This gives a self consistent explanation for the power law fitting of the ES gap. What's more, we also extract the dispersion power  $s$  for different  $g$  with  $L = 40$ . As Fig.4 (f) shows,  $s$  is close to 0.8 for  $g < 0.6035$  in the AKLT state, where the long-range term is irrelevant. When bulk approaches the quantum critical point and enter into the Néel phase,  $s$  decays very fast and finally decrease to 0.2, which indicates that long-range term becomes relevant and important near the entanglement boundary. It supports that the EH suddenly becomes long-range interacting after the ground state of

original Hamiltonian enters the gapless Néel phase from the gapped AKLT phase.

#### IV. WORLDLINE DECONFINEMENT

When the system is in the deep AKLT state, the EH can be considered as an  $S = 1/2$  short-ranged Heisenberg chain. Thus, the ES hosts gapless two-spinon excitation which is similar to a Heisenberg chain. Even if the boundary become gapped, the ES also looks like the edge energy spectrum, which can be explained by worm-hole picture [47]. When the bulk is gapped, the edge mode plays an important role in the ES because it has smaller cost and larger weight in the replica manifold. When the bulk goes into the gapless phase, the gapless bulk also provides the convenient path with small cost for worldlines to cross the replica and go for a long distance. It may induce the non-local interaction of EH.

We propose a new wormhole mechanism to explain the emergent long-range interaction, which is called worldline confinement/deconfinement. The effective long-range interaction can be regarded as the range worldline can go. In the AKLT phase, the EH is short-ranged. This demonstrates that a worldline only connect two spins at different time which are very close to each other locally. If a worldline want to go for a far distance, it needs a huge energy cost, which is worldline confinement. When the system is at quantum critical point or in the Néel phase,

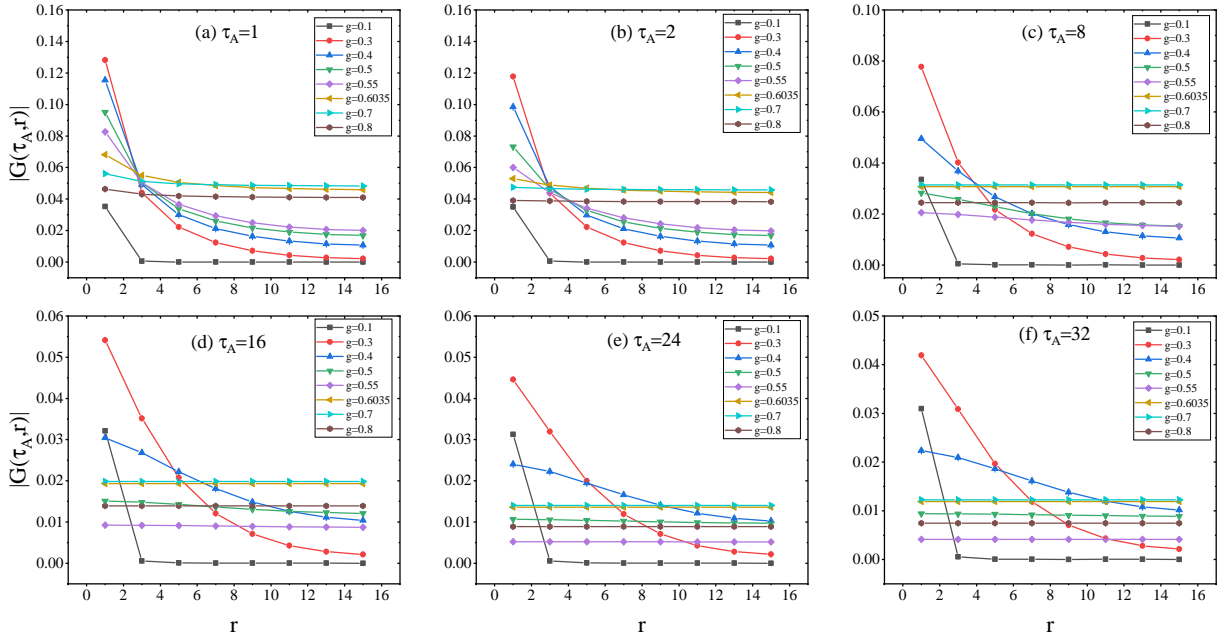


FIG. 5. Imaginary-time correlation function on the real space for different  $g$  with fixed  $\tau_A = 1(a), 2(b), 8(c), 16(d), 24(e)$  and  $32(f)$ .

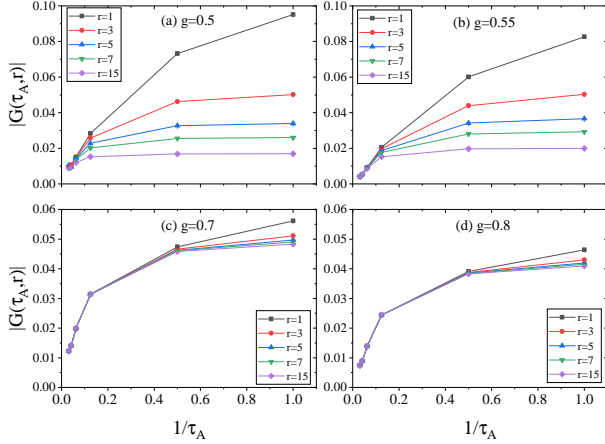


FIG. 6. Finite imaginary-time extrapolation of imaginary-time correlation function on the real space for  $g = 0.5$  (a),  $0.55$  (b),  $0.7$  (c) and  $0.8$  (d) with fixed  $r$ .

the worldline will connect two spins that are far away from each other with smaller cost, which is called worldline deconfinement. A worldline connecting two spins can be considered as an imaginary-time off-diagonal operator  $S^+(\tau, r)S^-(0, 0)$  and  $S^-(\tau, r)S^+(0, 0)$ , which flip the spins with different time and location. Its average is the imaginary-time off-diagonal correlation. Due to the  $SU(2)$  symmetry for the EH, we can measure the diagonal correlation  $|G(\tau_A, r)| = |\langle S^z(\tau_A, r)S^z(0, 0) \rangle|$  to detect the worldline confinement and deconfinement, since the diagonal correlation  $S^z(\tau, r)S^z(0, 0) = \frac{1}{4}[S^+(\tau, r)S^-(0, 0) + S^-(\tau, r)S^+(0, 0)]$ . The relation be-

tween worldline and EH can be understood easily by the recently proposed scheme—sampling reduced density matrix through QMC [48]—in which the off-diagonal elements of the reduced density matrix are proportional to the sampling frequency of the worldline connecting the left and right vectors.

When  $\tau_A$  is small, the correlation function will decay very fast in the AKLT phase, while it decays to a constant when the original system is at critical point or in the Néel phase, as shown in Fig.5(a)-(b). This demonstrates that worldline is confined in the AKLT phase but becomes deconfined in the critical phase and Néel phase. However, this difference between AKLT phase and Néel phase becomes fuzzy when  $\tau_A$  is large. As shown in Fig.5(c)-(f), the imaginary-time correlation function gradually decays to a constant as  $\tau_A$  increases with  $g = 0.5$  and  $0.55$ . It is hard to distinguish the worldline confinement in the AKLT phase and deconfinement in the Néel phase from the correlation directly. Actually, the entanglement spectrum from QMC stimulation reflects the physical properties of large  $\tau_A$  in replica manifold. Therefore, we perform the finite imaginary-time scaling of correlation function to check whether the worldline develops order in the AKLT phase. As depicted in Fig.6, we find that the correlation function will slowly converge to 0 in the AKLT phase (e.g.,  $g = 0.5$  and  $0.55$ ), while it converges to a finite constant in the Néel phase. This further confirms that worldline is confined in the AKLT phase and becomes deconfined in the critical phase and Néel phase even when  $\tau_A \rightarrow \infty$ . Therefore, the emergent effective long-range interaction becomes relevant and important in the EH, which can be reflected

directly by the worldline behaviors.

## V. CONCLUSION

In summary, we investigate the ES of the two-dimensional AKLT model. From AKLT state to Néel phase, the ES gradually becomes M-shaped sharp magnon excitation from gapless two-spinon excitation. This change of ES is similar to the one-dimensional Heisenberg chain from short-range interaction to long-range interaction, which is numerically verified in our QMC results. Moreover, the dispersion does not keep linear and becomes sublinear with power  $s < 1$  in the ES, which is also similar to the case in the one-dimensional Heisenberg chain with long-range interaction. The ES gap at  $q = \pi - 2\pi/L$  is nearly open but actually converges to 0 in the thermodynamic limit, which indicates the long-range interaction of EH plays a crucial role at both the quantum critical point and in the Néel phase of the original systems. Our results demonstrate that the long-range interaction can play an important role in the EH and ES which can not be ignored in the gapless phase. Furthermore, the emergent long-range interaction of EH

can be understood by the worldline deconfinement.

## VI. ACKNOWLEDGEMENTS

We thank F. Assaad and Z. Y. Meng for helpful discussions. D.X.Y. is supported by NKRDPC2022YFA1402802, NSFC-92165204, NSFC 12494591, Guangdong Provincial Key Laboratory of Magnetoelectric Physics and Devices (No.2022B1212010008), Research Center for Magnetoelectric Physics of Guangdong Province (No. 2024B0303390001), and Guangdong Provincial Quantum Science Strategic Initiative (No. GDZX2401010). Z.L. is supported by the China Postdoctoral Science Foundation under Grants No.2024M762935 and NSFC Special Fund for Theoretical Physics under Grants No.12447119. Z.W. is supported by the China Postdoctoral Science Foundation under Grant No. 2024M752898. The work is supported by the the Scientific Research Project (No.WU2024B027) and start-up funding of Westlake University. The authors thank the high-performance computing center of Westlake University and Beijing PARATERA Tech Co.,Ltd. for providing HPC resources.

- 
- [1] P. Calabrese and A. Lefevre, Entanglement spectrum in one-dimensional systems, *Phys. Rev. A* **78**, 032329 (2008).
- [2] E. Fradkin and J. E. Moore, Entanglement entropy of 2d conformal quantum critical points: Hearing the shape of a quantum drum, *Phys. Rev. Lett.* **97**, 050404 (2006).
- [3] Z. Nussinov and G. Ortiz, Sufficient symmetry conditions for Topological Quantum Order, *Proc. Nat. Acad. Sci.* **106**, 16944 (2009).
- [4] Z. Nussinov and G. Ortiz, A symmetry principle for topological quantum order, *Annals Phys.* **324**, 977 (2009).
- [5] H. Casini and M. Huerta, Universal terms for the entanglement entropy in 2+1 dimensions, *Nuclear Physics B* **764**, 183 (2007).
- [6] W. Ji and X.-G. Wen, Noninvertible anomalies and mapping-class-group transformation of anomalous partition functions, *Phys. Rev. Research* **1**, 033054 (2019).
- [7] W. Ji and X.-G. Wen, Categorical symmetry and noninvertible anomaly in symmetry-breaking and topological phase transitions, *Phys. Rev. Research* **2**, 033417 (2020).
- [8] L. Kong, T. Lan, X.-G. Wen, Z.-H. Zhang, and H. Zheng, Algebraic higher symmetry and categorical symmetry: A holographic and entanglement view of symmetry, *Phys. Rev. Research* **2**, 043086 (2020).
- [9] X.-C. Wu, W. Ji, and C. Xu, Categorical symmetries at criticality, *Journal of Statistical Mechanics: Theory and Experiment* **2021**, 073101 (2021).
- [10] X.-C. Wu, C.-M. Jian, and C. Xu, Universal features of higher-form symmetries at phase transitions, *SciPost Phys.* **11**, 33 (2021).
- [11] J. Zhao, Y.-C. Wang, Z. Yan, M. Cheng, and Z. Y. Meng, Scaling of entanglement entropy at deconfined quantum criticality, *Phys. Rev. Lett.* **128**, 010601 (2022).
- [12] J. Zhao, B.-B. Chen, Y.-C. Wang, Z. Yan, M. Cheng, and Z. Y. Meng, Measuring rényi entanglement entropy with high efficiency and precision in quantum monte carlo simulations, *npj Quantum Materials* **7**, 1 (2022).
- [13] Y.-C. Wang, N. Ma, M. Cheng, and Z. Y. Meng, Scaling of the disorder operator at deconfined quantum criticality, *SciPost Phys.* **13**, 123 (2022).
- [14] C. Holzhey, F. Larsen, and F. Wilczek, Geometric and renormalized entropy in conformal field theory, *Nuclear Physics B* **424**, 443 (1994).
- [15] P. Calabrese and J. Cardy, Entanglement entropy and quantum field theory, *Journal of Statistical Mechanics: Theory and Experiment* **2004**, P06002 (2004).
- [16] G. Vidal, J. I. Latorre, E. Rico, and A. Kitaev, Entanglement in quantum critical phenomena, *Phys. Rev. Lett.* **90**, 227902 (2003).
- [17] V. E. Korepin, Universality of entropy scaling in one dimensional gapless models, *Phys. Rev. Lett.* **92**, 096402 (2004).
- [18] A. Kitaev and J. Preskill, Topological entanglement entropy, *Phys. Rev. Lett.* **96**, 110404 (2006).
- [19] M. Levin and X.-G. Wen, Detecting topological order in a ground state wave function, *Phys. Rev. Lett.* **96**, 110405 (2006).
- [20] M. B. Hastings, I. González, A. B. Kallin, and R. G. Melko, Measuring renyi entanglement entropy in quantum monte carlo simulations, *Phys. Rev. Lett.* **104**, 157201 (2010).
- [21] A. B. Kallin, E. M. Stoudenmire, P. Fendley, R. R. P. Singh, and R. G. Melko, Corner contribution to the entanglement entropy of an o(3) quantum critical point in

- 2 + 1 dimensions, *Journal of Statistical Mechanics: Theory and Experiment* **2014**, P06009 (2014).
- [22] S. V. Isakov, M. B. Hastings, and R. G. Melko, Topological entanglement entropy of a bose-hubbard spin liquid, *Nature Physics* **7**, 772 (2011).
- [23] Y. Zhang, T. Grover, and A. Vishwanath, Topological entanglement entropy of  $F_2$  spin liquids and lattice Laughlin states, *Phys. Rev. B* **84**, 075128 (2011).
- [24] F. Pollmann, A. M. Turner, E. Berg, and M. Oshikawa, Entanglement spectrum of a topological phase in one dimension, *Phys. Rev. B* **81**, 064439 (2010).
- [25] L. Fidkowski, Entanglement spectrum of topological insulators and superconductors, *Phys. Rev. Lett.* **104**, 130502 (2010).
- [26] H. Yao and X.-L. Qi, Entanglement entropy and entanglement spectrum of the Kitaev model, *Phys. Rev. Lett.* **105**, 080501 (2010).
- [27] X.-L. Qi, H. Katsura, and A. W. W. Ludwig, General relationship between the entanglement spectrum and the edge state spectrum of topological quantum states, *Phys. Rev. Lett.* **108**, 196402 (2012).
- [28] E. Canovi, E. Ercolessi, P. Naldesi, L. Taddia, and D. Vodola, Dynamics of entanglement entropy and entanglement spectrum crossing a quantum phase transition, *Phys. Rev. B* **89**, 104303 (2014).
- [29] D. J. Luitz, N. Laflorencie, and F. Alet, Participation spectroscopy and entanglement hamiltonian of quantum spin models, *Journal of Statistical Mechanics: Theory and Experiment* **2014**, P08007 (2014).
- [30] D. J. Luitz, F. Alet, and N. Laflorencie, Shannon-rényi entropies and participation spectra across three-dimensional  $o(3)$  criticality, *Phys. Rev. B* **89**, 165106 (2014).
- [31] D. J. Luitz, F. Alet, and N. Laflorencie, Universal behavior beyond multifractality in quantum many-body systems, *Phys. Rev. Lett.* **112**, 057203 (2014).
- [32] C.-M. Chung, L. Bonnes, P. Chen, and A. M. Läuchli, Entanglement spectroscopy using quantum monte carlo, *Phys. Rev. B* **89**, 195147 (2014).
- [33] H. Pichler, G. Zhu, A. Seif, P. Zoller, and M. Hafezi, Measurement protocol for the entanglement spectrum of cold atoms, *Phys. Rev. X* **6**, 041033 (2016).
- [34] J. I. Cirac, D. Poilblanc, N. Schuch, and F. Verstraete, Entanglement spectrum and boundary theories with projected entangled-pair states, *Phys. Rev. B* **83**, 245134 (2011).
- [35] V. M. Stojanović, Entanglement-spectrum characterization of ground-state nonanalyticities in coupled excitation-phonon models, *Phys. Rev. B* **101**, 134301 (2020).
- [36] W.-z. Guo, Entanglement spectrum of geometric states, *Journal of High Energy Physics* **2021**, 1 (2021).
- [37] T. Grover, Entanglement of interacting fermions in quantum monte carlo calculations, *Phys. Rev. Lett.* **111**, 130402 (2013).
- [38] F. F. Assaad, T. C. Lang, and F. Parisen Toldin, Entanglement spectra of interacting fermions in quantum monte carlo simulations, *Phys. Rev. B* **89**, 125121 (2014).
- [39] F. F. Assaad, Stable quantum monte carlo simulations for entanglement spectra of interacting fermions, *Phys. Rev. B* **91**, 125146 (2015).
- [40] F. Parisen Toldin and F. F. Assaad, Entanglement hamiltonian of interacting fermionic models, *Phys. Rev. Lett.* **121**, 200602 (2018).
- [41] X.-J. Yu, R.-Z. Huang, H.-H. Song, L. Xu, C. Ding, and L. Zhang, Conformal boundary conditions of symmetry-enriched quantum critical spin chains, *Phys. Rev. Lett.* **129**, 210601 (2022).
- [42] H. Li and F. D. M. Haldane, Entanglement spectrum as a generalization of entanglement entropy: Identification of topological order in non-abelian fractional quantum hall effect states, *Phys. Rev. Lett.* **101**, 010504 (2008).
- [43] D. Poilblanc, Entanglement spectra of quantum heisenberg ladders, *Phys. Rev. Lett.* **105**, 077202 (2010).
- [44] Z. Yan and Z. Y. Meng, Unlocking the general relationship between energy and entanglement spectra via the wormhole effect, *Nature Communications* **14**, 2360 (2023).
- [45] W. Zhu, Z. Huang, and Y.-C. He, Reconstructing entanglement hamiltonian via entanglement eigenstates, *Phys. Rev. B* **99**, 235109 (2019).
- [46] J. Lou, S. Tanaka, H. Katsura, and N. Kawashima, Entanglement spectra of the two-dimensional affleck-kennedy-lieb-tasaki model: Correspondence between the valence-bond-solid state and conformal field theory, *Phys. Rev. B* **84**, 245128 (2011).
- [47] Z. Liu, R.-Z. Huang, Z. Yan, and D.-X. Yao, Demonstrating the wormhole mechanism of the entanglement spectrum via a perturbed boundary, *Phys. Rev. B* **109**, 094416 (2024).
- [48] B.-B. Mao, Y.-M. Ding, Z. Wang, S. Hu, and Z. Yan, Sampling reduced density matrix to extract fine levels of entanglement spectrum and restore entanglement hamiltonian, *Nature Communications* **16**, 2880 (2025).
- [49] X.-L. Qi, H. Katsura, and A. W. W. Ludwig, General relationship between the entanglement spectrum and the edge state spectrum of topological quantum states, *Phys. Rev. Lett.* **108**, 196402 (2012).
- [50] R. Lundgren, Y. Fuji, S. Furukawa, and M. Oshikawa, Entanglement spectra between coupled Tomonaga-Luttinger liquids: Applications to ladder systems and topological phases, *Phys. Rev. B* **88**, 245137 (2013).
- [51] M. Dalmonte, V. Eisler, M. Falconi, and B. Vermersch, Entanglement hamiltonians: from field theory to lattice models and experiments, *Annalen der Physik* **534**, 2200064 (2022).
- [52] G. Giudici, T. Mendes-Santos, P. Calabrese, and M. Dalmonte, Entanglement hamiltonians of lattice models via the Bisognano-Wichmann theorem, *Physical Review B* **98**, 134403 (2018).
- [53] M. Dalmonte, B. Vermersch, and P. Zoller, Quantum simulation and spectroscopy of entanglement hamiltonians, *Nature Physics* **14**, 827 (2018).
- [54] S. Wu, X. Ran, B. Yin, Q.-F. Li, B.-B. Mao, Y.-C. Wang, and Z. Yan, Classical model emerges in quantum entanglement: Quantum monte carlo study for an Ising-Heisenberg bilayer, *Phys. Rev. B* **107**, 155121 (2023).
- [55] M. Song, J. Zhao, Z. Yan, and Z. Y. Meng, Different temperature dependence for the edge and bulk of the entanglement hamiltonian, *Physical Review B* **108**, 075114 (2023).
- [56] T. Yoshino, S. Furukawa, and M. Ueda, Intercomponent entanglement entropy and spectrum in binary Bose-Einstein condensates, *Phys. Rev. A* **103**, 043321 (2021).
- [57] C. Li, R.-Z. Huang, Y.-M. Ding, Z. Y. Meng, Y.-C. Wang, and Z. Yan, Relevant long-range interaction of the entanglement hamiltonian emerges from a short-range gapped system (2024).

- [58] Z. Wang, S. Yang, B.-B. Mao, M. Cheng, and Z. Yan, Sudden change in entanglement hamiltonian: Phase diagram of an ising entanglement hamiltonian (2024), arXiv:2410.10090 [cond-mat.str-el].
- [59] N. D. Mermin and H. Wagner, Absence of ferromagnetism or antiferromagnetism in one- or two-dimensional isotropic heisenberg models, *Phys. Rev. Lett.* **17**, 1133 (1966).
- [60] N. D. Mermin, Absence of ordering in certain classical systems, *Journal of Mathematical Physics* **8**, 1061 (1967).
- [61] M. Song, J. Zhao, C. Zhou, and Z. Y. Meng, Dynamical properties of quantum many-body systems with long-range interactions, *Physical Review Research* **5**, 033046 (2023).
- [62] M. Song, J. Zhao, Y. Qi, J. Rong, and Z. Y. Meng, Quantum criticality and entanglement for the two-dimensional long-range heisenberg bilayer, *Phys. Rev. B* **109**, L081114 (2024).
- [63] J. Zhao, M. Song, Y. Qi, J. Rong, and Z. Y. Meng, Finite-temperature critical behaviors in 2d long-range quantum heisenberg model, *npj Quantum Materials* **8**, 59 (2023).
- [64] O. K. Diessel, S. Diehl, N. Defenu, A. Rosch, and A. Chiochetta, Generalized higgs mechanism in long-range-interacting quantum systems, *Phys. Rev. Res.* **5**, 033038 (2023).
- [65] N. Defenu, T. Donner, T. Macrì, G. Pagano, S. Ruffo, and A. Trombettoni, Long-range interacting quantum systems, *Rev. Mod. Phys.* **95**, 035002 (2023).
- [66] I. Affleck, T. Kennedy, E. H. Lieb, and H. Tasaki, Rigorous results on valence-bond ground states in antiferromagnets, *Phys. Rev. Lett.* **59**, 799 (1987).
- [67] L. Zhang and F. Wang, Unconventional surface critical behavior induced by a quantum phase transition from the two-dimensional affleck-kennedy-lieb-tasaki phase to a néel-ordered phase, *Physical Review Letters* **118**, 087201 (2017).
- [68] Z. Liu, J. Li, R.-Z. Huang, J. Li, Z. Yan, and D.-X. Yao, Bulk and edge dynamics of a two-dimensional affleck-kennedy-lieb-tasaki model, *Phys. Rev. B* **105**, 014418 (2022).
- [69] Z. Liu, R.-Z. Huang, Y.-C. Wang, Z. Yan, and D.-X. Yao, Measuring the boundary gapless state and criticality via disorder operator, *Phys. Rev. Lett.* **132**, 206502 (2024).
- [70] A. W. Sandvik, Constrained sampling method for analytic continuation, *Phys. Rev. E* **94**, 063308 (2016).
- [71] H. Shao and A. W. Sandvik, Progress on stochastic analytic continuation of quantum monte carlo data, *Physics Reports* **1003**, 1 (2023).
- [72] C. Zhou, Z. Yan, H.-Q. Wu, K. Sun, O. A. Starykh, and Z. Y. Meng, Amplitude mode in quantum magnets via dimensional crossover, *Phys. Rev. Lett.* **126**, 227201 (2021).
- [73] Z. Yan, Y.-C. Wang, N. Ma, Y. Qi, and Z. Y. Meng, Topological phase transition and single/multi anyon dynamics of z 2 spin liquid, *npj Quantum Materials* **6**, 39 (2021).
- [74] N. Laflorencie, I. Affleck, and M. Berciu, Critical phenomena and quantum phase transition in long range heisenberg antiferromagnetic chains, *Journal of Statistical Mechanics: Theory and Experiment* **2005**, P12001 (2005).
- [75] J. Zhao, N. Laflorencie, and Z. Y. Meng, Unconventional scalings of quantum entropies in long-range heisenberg chains, *Phys. Rev. Lett.* **134**, 016707 (2025).
- [76] E. Yusuf, A. Joshi, and K. Yang, Spin waves in antiferromagnetic spin chains with long-range interactions, *Phys. Rev. B* **69**, 144412 (2004).
- [77] O. K. Diessel, S. Diehl, N. Defenu, A. Rosch, and A. Chiochetta, Generalized higgs mechanism in long-range interacting quantum systems (2022), arXiv:2208.10487 [cond-mat.quant-gas].
- [78] E. Lieb and D. Mattis, Ordering energy levels of interacting spin systems, *Journal of Mathematical Physics* **3**, 749 (1962), [https://pubs.aip.org/aip/jmp/article-pdf/3/4/749/19167430/749\\_1\\_online.pdf](https://pubs.aip.org/aip/jmp/article-pdf/3/4/749/19167430/749_1_online.pdf).
- [79] S. Yang, G. Schumm, and A. W. Sandvik, Dynamic structure factor of a spin-1/2 heisenberg chain with long-range interactions (2024), arXiv:2412.15168 [cond-mat.str-el].